

FROSCOEZA



12 JUN 1995

ORK



LAPP-EXP-94.27

## Neutrino Oscillation : Status and Outlooks

Patrick NEDELEC\*

*Laboratoire d'Annecy-le-Vieux de Physique des Particules  
Chemin de Bellevue  
BP110, 74941 Annecy-le-Vieux, France*

### ABSTRACT

Whether the neutrinos are massive or not is one of the most puzzling question of physics today. If they are massive, they can contribute significantly to the Dark Matter of the Universe. An other consequence of a non-zero mass of neutrinos is that they might oscillate from one flavor to another. This oscillation process is by now the only way to detect a neutrino with a mass in the few eV range. Several neutrino experiments are currently looking for such an oscillation, in different modes, using different technics. In this paper, we give an overview of the experimental situation for neutrino experiments at accelerators.

Talk given at the 2<sup>nd</sup> Tennessee International Symposium on Radiative Corrections  
June 27 - July 01, 1994  
Gatlinburg, Tennessee, USA

\*e-mail address : nedelec@axnd02.cern.ch

VOL 26 No 2 2

# Neutrino Oscillation : Status and Outlooks

Patrick NEDELEC

*Laboratoire d'Annecy-le-Vieux de Physique des Particules  
Chemin de Bellevue  
Annecy-le-Vieux, France*

## ABSTRACT

Whether the neutrinos are massive or not is one of the most puzzling question of today physics. If they are massive, they can contribute significantly to the Dark Matter of the Universe. An other consequence of a non-zero mass of neutrinos is that they might oscillate from one flavor to another. This oscillation process by now the only way to detect a neutrino with a mass in the few eV range. Several neutrino experiments are currently looking for such an oscillation, in different modes, using different technics. In this paper, we give an overview of the experimental situation for neutrino experiments at accelerators.

## 1. Introduction

The neutrino particle has been introduced in Particle Physics a long time ago (1930's) by W. Pauli, in order to solve the problem of  $\beta$  decay spectrum as well as to save the energy momentum conservation law<sup>1</sup>. The neutrino was described as a neutral, light or even massless, fermion.

The first neutrino, the  $\nu_e$ , was discovered in 1954<sup>2</sup>, and the second one, the  $\nu_\mu$ , in 1962. The direct detection of the third generation of neutrino, the  $\nu_\tau$ , has not yet occured, but its existence is of no doubt.

More recently the four LEP experiments have settled a limit on the number of light neutrino species ( $m_\nu \leq m_Z/2$ ) compatible with only three flavors ( $N_\nu = 2.988 \pm 0.023$ ). On the other hand, cosmological studies give also a limit on the number of neutrino species ( $N_\nu < 3.6$ ). So it is quite probable that only three light neutrino species exist.

The most exciting question about these three neutrinos, is the value of their masses. A non zero mass value would be an evidence of physics beyond the Standard Model.

An important consequence of a non zero value of the neutrino masses, is due to their contributions to the total energy density of the Universe. Assuming a  $\nu_\tau$  mass of a few tens of eV, and a hierarchy of masses, where the  $\nu_\tau$  is the heaviest neutrino, and according to a mean density of  $110 \nu'/\text{cm}^3$ , it is possible to reach the critical density, leading to a flat Universe, and consequently solve in a simple way the problem of the Dark Matter.

Experimentally, the search for neutrino masses can be performed in two ways : either to look at the end point spectrum of beta decays, or to measure their contributions to the neutrino oscillation mechanism.

## 2. Are $\nu$ 's massive ?

The direct mass limits are based on the kinematical constraints that can be set on weak decay spectrum. The following table shows the current experimental direct limits obtained on the masses of the  $\bar{\nu}_e$ , the  $\nu_e$ , the  $\nu_\mu$  and the  $\nu_\tau$ , as quoted at the last Neutrino conference (Eilat,  $\nu$ 's 94).

neutrino type	mass limits	Reactions
$\bar{\nu}_e$	$m_{\bar{\nu}_e} < 4.0 \text{ eV}$	${}^3\text{H} \rightarrow {}^3\text{He} + e^- + \bar{\nu}_e$
$\nu_e$	$m_{\nu_e} < 500. \text{ eV}$	${}^{163}\text{Ho} + e^- \rightarrow \text{Dy} + \gamma + \nu_e$
$\nu_\mu$	$m_{\nu_\mu} < 220. \text{ keV}$	$\pi^+ \rightarrow \mu^+ + \nu_\mu$
$\nu_\tau$	$m_{\nu_\tau} < 31. \text{ MeV}$	$\tau^- \rightarrow 5\pi + \nu_\tau$

Table 1: Neutrino mass limits and their mode of production

In the framework of the Standard Model the neutrinos are massless particles. It would be interesting to understand why the neutral elementary fermions behave differently than the charged ones. Are the masses of fermions related to their charge ? Or is there a very deep reason for neutrino to be massless ? This is still unanswered questions.

Theoretically, a simple and elegant way to give mass to neutrinos is the *see-saw* mechanism<sup>3</sup>, in which the neutrino masses are related to the mass of the charged partners via a simple relation :

$$m_\nu \times M \propto m_q^2, m_l^2 \text{ or } m_q$$

where  $M$  is related to the Grand Unification scale  $M_{GUT}$ .

Massive neutrinos are also expected to decay ( $\nu_i \rightarrow \nu_j + \gamma$ ). They could also have a magnetic moment, and depending on the very nature of this fermion (Majorana or Dirac) one should expect neutrinoless  $\beta$ -decay ( $\beta\beta 0\nu$ ) to occur.

An interesting feature of massive neutrinos is related to the possibility for the neutrinos to evolve with time from one state to an other one via the neutrino oscillation mechanism.

## 3. $\nu$ 's oscillation

The neutrino oscillation idea was formerly proposed by B. Pontecorvo between neutrinos and anti-neutrinos. He soon realised that such a mechanism is also valid between different neutrino species. Two conditions are required for oscillation to occur :

- It exists at least two neutrino states with different masses :  
 $\Delta m^2 = (m_i - m_j)^2 \neq 0$
- It exists a mixing angle matrix  $U_{ij}$ .

If we restrict ourselves to the case of two neutrino flavors, we can write the transition probability for neutrino  $i$  to become a neutrino  $j$  after travelling a distance  $L$  as :

$$P(\nu_i \rightsquigarrow \nu_j) = \sin^2 2\theta \times \sin^2(2\pi \frac{L}{\lambda})$$

where  $\sin \theta = U_{ij}$  is the mixing angle and

$$\lambda(\text{km}) = 5 \frac{E_\nu(\text{GeV})}{\Delta m^2(\text{eV}^2)}$$

is the oscillation length, where  $E_i$  is the neutrino energy. One should rewrite the transition probability as :

$$P(\nu_i \rightsquigarrow \nu_j) = a \times \sin^2(1.27 \frac{L(\text{m/km})}{E_\nu(\text{MeV/GeV})} \Delta m^2(\text{eV}^2))$$

The oscillation probability depends upon two parameters :  $\sin^2 2\theta$  and  $\Delta m^2$ . The sensitivity on  $\sin^2 2\theta$  is only dependant on the accumulated statistics of the experiment. The sensitivity of  $\Delta m^2$  is very dependant of  $\frac{L}{E_\nu}$ , which characterises the experimental set-up. When no neutrino oscillation is found (this happens quite often !) one express oscillation limits by exclusion zones in the well known oscillation plane ( $\Delta m^2, \sin^2 2\theta$ ).

The mass sensitivity of an experiment is given at the limit for a full mixing ( $\sin^2 2\theta = 1$ ) for which  $\Delta m^2 \geq E_\nu/L$ .

When the detector size  $d$  becomes large compared to the oscillation length ( $\Delta m^2 > 5E_\nu/d$ ) the oscillation can occur everywhere in the detector, and the factor  $\sin^2(2\pi \frac{L}{\lambda})$  averages to  $\frac{1}{2}$ . This is the limit of large  $\Delta m^2$ .

Different sources of neutrino can be used for neutrino oscillation experiments, with energies ranging from few 100 keV up to several hundreds GeV, and with distances source-detector  $L$  varying from 10 m up to 150 million km (1 AU). So far the oscillation length can then be studied between  $10^{-2}$  to  $10^{11}$  km/GeV.

Actually, it is not possible for one experiment to be sensitive to the full plane ( $\Delta m^2, \sin^2 2\theta$ ), so different kinds of neutrino oscillation experiments have been proposed, using different neutrino sources such as the sun, the atmosphere, the nuclear reactors or the accelerator beams as described below.

**Solar neutrinos** <sup>6</sup> are produced in the solar core when hydrogen burns into helium via the so-called solar cycle :  $4p \rightarrow {}^4\text{He} + 2e^- + 2\nu_e + 27 \text{ MeV}$ .

The energy spectrum of the interacting neutrinos are in the range 100 keV to 20 MeV, and the distance 1 AU.

The rate of  $\nu_e$  interaction produced is compared with the standard solar model predictions. Any deficit might be interpreted in terms of  $\nu_e \rightsquigarrow \nu_x$  oscillation (disappearance experiment), including matter effect in the sun (MSW effect).

**Atmospheric neutrinos** <sup>7</sup> are among the final decay products of the  $\pi^\pm$  and  $K^\pm$  present in the showers produced during the interactions of cosmic rays in the high atmosphere :

$$\pi^\pm \rightarrow \mu^\pm \nu_\mu \quad \text{and} \quad \mu^\pm \rightarrow e^\pm \nu_\mu \nu_e$$

Their energies are in the range 0.1 to 2 GeV, for distances between 10 and 10.000 km. According to the two reactions above, the ratio  $N(\nu_\mu)/N(\nu_e)$  is expected to be about 2. It has been measured in deep underground experiments, and found to be 0.6 times the theoretical expectation. This apparent discrepancy should be interpreted in terms of  $\nu_\mu \rightsquigarrow \nu_e$  oscillations (disappearance experiment).

**Reactor neutrinos** <sup>8</sup> are produced by nuclear reactors through fission reactions of uranium or plutonium :  $U/P \rightarrow \bar{\nu}_e$ . Their energies vary about 2 and 10 MeV, while the distance  $L$  should vary between 10 and few hundred meters. Once more, any discrepancy between the measured and the expected fluxes, might be interpreted in terms of  $\bar{\nu}_e \rightsquigarrow \bar{\nu}_\mu$  oscillation (disappearance experiment).

**Accelerator neutrinos** are produced by smashing high energy protons on a fixed target. Depending on the proton energy, and selecting a defined charge by magnetic deflectors, one can produce a rather pure neutrino beam.

In *medium* energy experiments the incident proton has an energy of several 100 MeV, leading to the production of  $\nu_\mu$ ,  $\nu_e$  and  $\bar{\nu}_e$ .

In *high* energy experiments, the incident protons have several hundred GeV. The main neutrino component is the  $\nu_\mu$ , but  $\bar{\nu}_\mu$ ,  $\nu_e$  and  $\bar{\nu}_e$  are also present.

In both kind of experiments, the search for neutrino oscillations (appearance experiments), is performed through events that are not expected to occur in the interactions from neutrino contained in the beam.

In the following section, we review the current accelerator experiments.

#### 4. Medium energy experiments

Two experiments in the *medium* energy range are actually taking data. LNSD at LAMPF (Los Alamos) and KARMEN at ISIS (Rutherford).

These experiments are both looking for the oscillations  $\nu_\mu \rightsquigarrow \nu_e$  and  $\bar{\nu}_\mu \rightsquigarrow \bar{\nu}_e$  using liquid scintillator detectors. The difference in decay times for the  $\pi$ 's and the  $\mu$ 's are used in both case to separate  $\nu_\mu$  and  $\bar{\nu}_\mu$  interactions.

##### 4.1. LNSD

LSND (Liquid Scintillator Neutrino Detector) is a large cylindrical tank (8.5 m long, 5.5 m in diameter) filled with 180 tons of liquid scintillator<sup>9</sup>. It is located 29 m

downstream a beam stopper and is well shielded against beam and cosmic rays. The inner surface of the tank is equipped with 1220 photomultipliers which collect both the Čerenkov and the scintillation light. For particles above Čerenkov threshold, the Čerenkov cone can be reconstructed. This measurement of the energy and a good time resolution allows to separate electrons from protons and muons.

The pion beam, is produced by a 780 MeV proton beam, giving rise to a  $\nu_\mu$  beam of energy in the range  $30 < E_{\nu_\mu} < 250$  MeV, with a mean value around 100 MeV. The total intensity recorded by the experiment since September 1993 corresponds to 1813 Coulomb ( $1.13 \cdot 10^{22}$  p.o.t's<sup>\*</sup>).

The search for neutrino oscillations is performed in the two following modes :

$\nu_\mu \rightsquigarrow \nu_e + {}^{12}\text{C} \rightarrow e^- + {}^{12}\text{N}$  : One demands a single electron in the detector, with energy in the range  $70 < E_{e^-} < 180$  MeV.

$\bar{\nu}_\mu \rightsquigarrow \bar{\nu}_e + p \rightarrow e^+ + n$  : In this channel, one requires a single positron in the ( $\bar{\nu}_\mu, \nu_e$ ) time window, with energy in the range  $37 < E_{e^+} < 56$  MeV, in coincidence with a 2.2 MeV  $\gamma$  ray coming from the neutron absorption on a free proton within 0.5 ms.

The analysis of the first channel is not complete (Eilat,  $\nu$ 's 94), so no limit have been set yet. Anyhow, the estimated background would amount to 13 events. If no excess of event is observed, this experiment should set a limit on the neutrino oscillation :

$$\sin^2 2\theta_{\mu e} > 2.7 \cdot 10^{-4} \text{ (@90\%CL) for } \Delta m_{\mu e}^2 > 3 \text{ eV}^2$$

In the  $\bar{\nu}_\mu \rightsquigarrow \bar{\nu}_e$  channel, a preliminary set of criteria selection yields 8 events with electron and photon energy in the expected range, for one event of background (Eilat,  $\nu$ 's 94).

#### 4.2. KARMEN

The KARMEN (Karlsruhe Rutherford Medium Energy Neutrino Experiment) is a large ( $3 \times 3.5 \times 6.5 \text{ m}^3$ ) calorimeter tank filled with 56 tons of liquid scintillator, containing 0.1% of Gadolinium (Gd) which ensures a high detection efficiency for neutrons. This calorimeter consists in  $560 \times 3.5$  m long cells, read out by two photomultipliers at both extremities. It is well shielded, and surrounded by vetoes, inside and outside the shielding. The energy and time resolutions are respectively  $\sigma(E)/E = 0.115/\sqrt{E(\text{MeV})}$  and  $\sigma(t) = 0.7$  ns.

The decay of pions at rest, produced in a  $U/D_2O$  target on the 800 MeV pulsed proton beam, yields monoenergetic  $\nu_\mu$ 's ( $E_{\nu_\mu} = 29.8$  MeV). The delayed muon decay produces the same fluxes of  $\bar{\nu}_\mu$  and  $\nu_e$ , with an energy end point at 52.8 MeV. The experiment is located 18 m downstream the target, at an angle of 12 degrees with

\*The proton on target (p.o.t) unit is preferently used for high energy neutrino beam :  
1 p.o.t =  $1.6 \cdot 10^{19}$  C

respect to the incident proton beam. The total intensity recorded by the experiment since July 1990 is 5670 C ( $3.5 \cdot 10^{22}$  p.o.t.'s).

This experiment is also looking at the two oscillation modes :

$\nu_\mu \rightsquigarrow \nu_e + {}^{12}\text{C} \rightarrow e^- + {}^{12}\text{N}_{gs}$  : To select these events one requires a monoenergetic 12.5 MeV electron ( $E_{e^-} = E_\nu - 17.3$  MeV), in a narrow time window around the beam on target signal. The  $\beta^+$  decay of the ground state  ${}^{12}\text{N}_{gs}$  releases a positron, which originates from the same position as the previous electron, and which is emitted in a time window compatible with the 16 ms desexcitation time.

$\bar{\nu}_\mu \rightsquigarrow \bar{\nu}_e + p \rightarrow e^+ + n$  : In this channel, one demands a single positron in the delayed ( $\bar{\nu}_\mu, \nu_e$ ) time window with energy in the range  $30 < E_{e^+} < 50$  MeV, followed by a delayed gamma rays emission from neutron capture on proton or Gd.

In the first channel, 3 events have been selected (159 are expected for a full mixing) for 4.3 background events expected. Converting the limit on the oscillation probability ( $P < 2.4 \cdot 10^{-2}$ ), one obtains :

$$\begin{aligned} \sin^2 2\theta_{\mu e} &< 4.8 \cdot 10^{-2} \text{ (@90\%CL) for large } \Delta m_{\mu e}^2 \\ \Delta m_{\mu e}^2 &< 0.2 \text{ eV}^2 \text{ for a full mixing angle} \end{aligned}$$

In the second channel, no event has been found for 0.4 background expected. The 90 % CL limit on oscillation probability is ( $P < 3.2 \cdot 10^{-2}$ ), which leads to the exclusion limits :

$$\begin{aligned} \sin^2 2\theta_{\mu e} &< 6.4 \cdot 10^{-3} \text{ (@90\%CL) for large } \Delta m_{\mu e}^2 \\ \Delta m_{\mu e}^2 &< 0.08 \text{ eV}^2 \text{ for a full mixing angle} \end{aligned}$$

In the future, the ISIS beam will deliver 3000 C per year.

## 5. High energy neutrino beams experiments

Two experiments NOMAD and CHORUS, both looking for the oscillation  $\nu_\mu \rightsquigarrow \nu_\tau$ , are taking data since the beginning of this year, using the wide band neutrino beam at CERN. They are two appearance experiments using a rather pure  $\nu_\mu$  beam. The search for neutrino oscillation is done via the identification of charged current events :

$$\begin{aligned} \nu_\tau + N &\rightarrow \tau^- + X \\ &\text{(reaction threshold 3.5 GeV)} \end{aligned}$$

The final  $\tau$  decay signature is extracted from the different backgrounds by applying purely kinematical selections (NOMAD), or by seeing the  $\tau$  track and its decay product (CHORUS).

### 5.1. The neutrino beam

The CERN neutrino beam is produced by a 450 GeV proton beam hitting a Be target. The outgoing charged particles are either focussed along the proton beam

axis, or deflected by a magnetic horn, according of their charge. A decay tunnel lets neutrino to be produced and an iron-earth absorber is then used to absorb all the other particles. The detectors are located about 800 m downstream the target.

The composition of the neutrino beam is summarised in the following table :

Neutrino type	Relative fraction (%)	$\langle E_\nu \rangle$ (GeV)	Production mode
$\nu_\mu$	100	26.7	$\pi^+$ and $K^+$ decays
$\bar{\nu}_\mu$	6	21.7	$\pi^-$ and $K^-$ decays
$\nu_e$	$\sim 0.7$	47.9	$K_{e3}^+$ decay
$\bar{\nu}_e$	$\sim 0.3$	35.3	$\mu$ decay
$\nu_\tau$	$< 10^{-7}$		$D_s \rightarrow \tau \nu_\tau$

Table 2: CERN neutrino beam composition : Relative fraction, mean energy and production mode

The nominal integrated luminosity is  $2.4 \cdot 10^{19}$  p.o.t.'s over two years. The integrated luminosity already collected is about  $0.8 \cdot 10^{19}$  p.o.t.'s.

## 5.2. NOMAD

The NOMAD (Neutrino Oscillation Magnetic Detector) experiment has been designed to distinguish the oscillation signal  $\nu_\tau + N \rightarrow \tau + X$  from the backgrounds by applying cuts on angular correlations, and on kinematical variables such as the missing transverse momentum ( $P_t^{miss}$ ). This is possible by using a high precision detector, with a good momentum, energy and direction resolution.

The experimental set-up<sup>4</sup> is a large volume tracker target ( $3 \times 3 \times 4 \text{ m}^3$ ) followed by a set of particle identification detectors sitting in the re-used UA1 magnet (see figure 1). The active target of this experiment (3 tons) consists of 44 chambers with three drift planes each, built of composite material. They are made with a honeycomb structure covered by Kevlar skin walls, where most of the target mass is located in the skins. The whole target amount for only one radiation length. The expected momentum resolution,  $\sigma(p)/p$ , for tracks of averaged length, ranges between 3 and 5 %. The horizontal magnetic field of 0.4 Tesla is perpendicular to the neutrino beam axis. The nominal resolution along the vertical drift axis is  $250 \mu\text{m}$ .

The particle identification set includes a transition radiation detector (TRD), used to separate electrons from hadrons. It consists in 9 modules, grouped by two, followed by a drift chamber. Each module includes a radiator made with 315 polypropylene foils,  $25 \mu\text{m}$  thick, located in front of a plane of straw tubes filled with a mixture Xenon-Methane, used to detect the transition radiation X-rays. The TRD is followed by a preshower detector, consisting of a lead plane and two perpendicular planes of tubes. It is located in front of the lead glass electromagnetic calorimeter



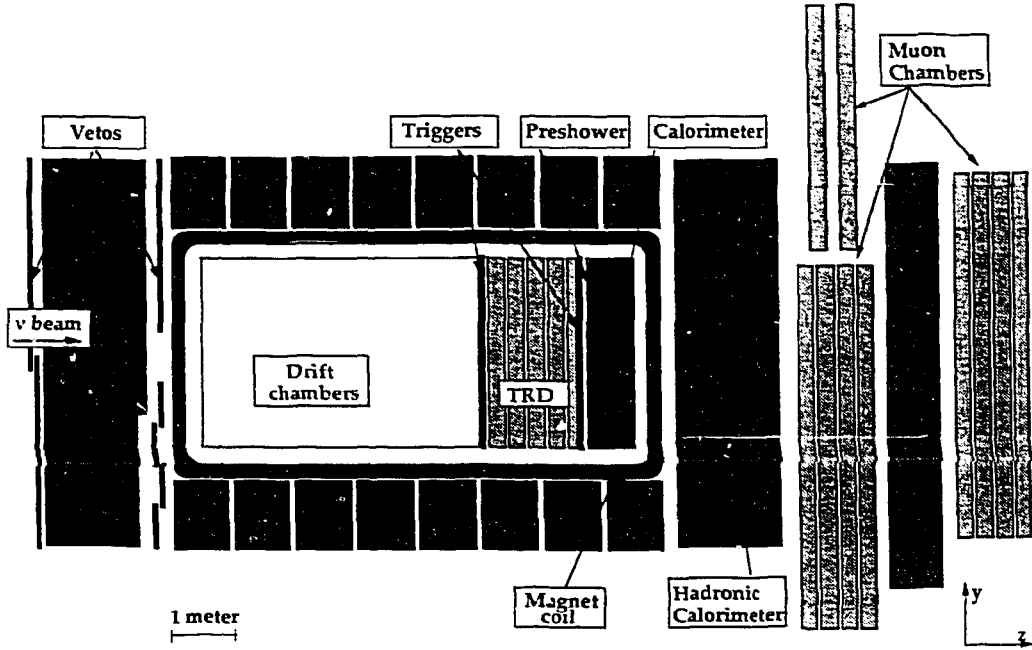


Figure 1: The NOMAD detector (side view)

which has a energy resolution  $\sigma(E)/E = 0.04/\sqrt{(E)} + 0.01$ . The preshower and the calorimeter also provide a way to further improve the electron pion separation, as well as to help at the localisation of bremsstrahlung photons emitted by electrons. The overall electron-pion separation is expected to be better than  $10^5$ .

Downstream, in the return coil, a hadronic calorimeter is currently under installation. Finally, outside the magnet, two sets of muon chambers separated by an iron shielding identify and measure the muons.

The trigger system consists in a veto plane and two trigger counters.

### 5.2.1. Event selection

The main idea for the event to background separation in NOMAD is to use the different topological and kinematical behaviour of the two kind of events. For illustration, we can look at the electronic decay of  $\tau$ . The main background comes from the 1% charged current interaction from  $\nu_e$  contained in the beam. One has to deal with the two processes :

$$\begin{aligned} \nu_\tau + N &\rightarrow \tau^- + X & \nu_e + N &\rightarrow e^- + X \\ \tau^- &\rightarrow e^- \bar{\nu}_e \nu_\tau & & \text{and} \end{aligned}$$

In the plane transverse to the beam, one defines the angle between the outgoing electron and the hadronic system  $\phi_{eh}$  and the angle between the missing transverse energy  $P_t^{miss}$  and the hadronic system  $\phi_{mh}$  (see figure 2):

In the case of an electronic  $\tau$  decay (fig. 2a), the hadrons ( $X$ ) are produced, in

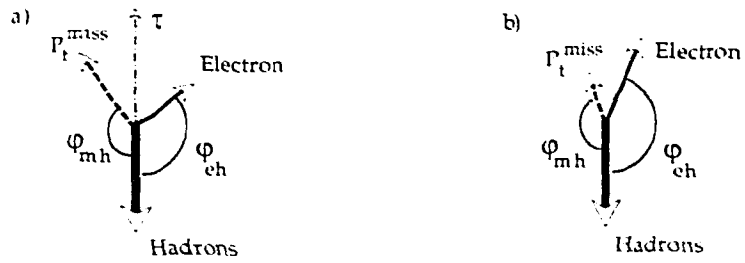


Figure 2: Definition of the angles  $\phi_{eh}$  and  $\phi_{mh}$ . a)  $\nu_\tau + N \rightarrow \tau + X$ , with  $\tau \rightarrow e^-$   
 $\nu_\tau \bar{\nu}_e$  b)  $\nu_e + N \rightarrow e^- \bar{\nu}_e$

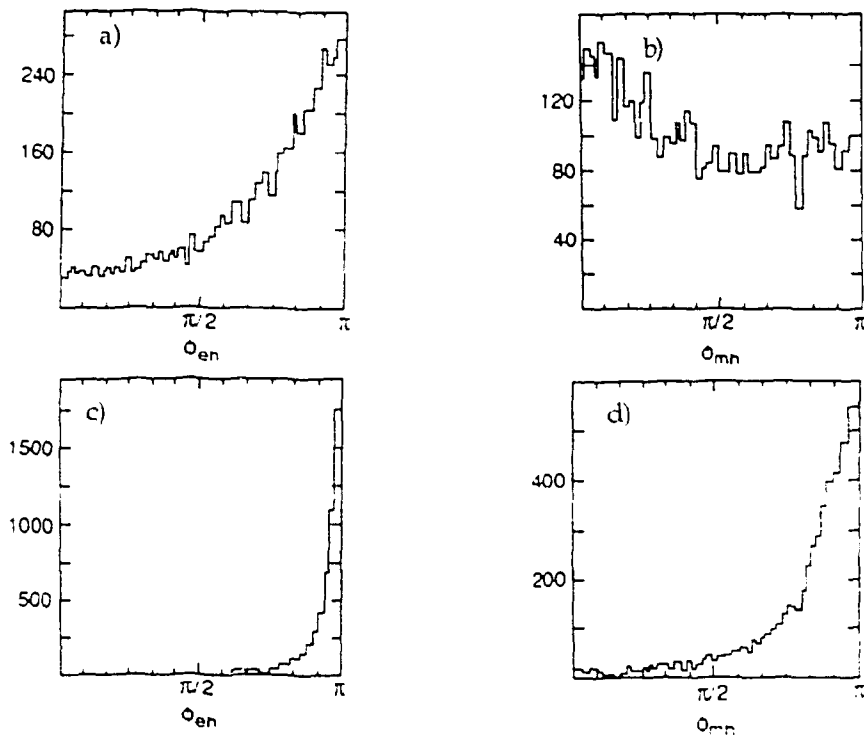


Figure 3: Angular distributions  $\phi_{eh}$  and  $\phi_{mh}$  for  $\nu_\tau$  CC (a and b, on top) and for  $\nu_e$  CC (c and d, on bottom).

the transverse plane, back to back to the  $\tau$ . The missing momentum  $\mathbf{P}_t^{miss}$  is the vectorial sum of the neutrino momenta. Summing-up  $\mathbf{P}_t^{miss}$  to the electron momentum gives the  $\tau$  momentum itself.

The figures 3a and 3b show the  $\phi_{eh}$  and  $\phi_{mh}$  distributions expected for such a process.

In the case of the  $\nu_e$  charged current interaction (fig. 2b), the electron is produced back to back to the hadron. No  $\mathbf{P}_t^{miss}$  is expected in such a process. However the limited resolution on both the energy and momentum measurements, as well as the unseen particles (neutron,  $K^0$ ) would fake a  $\mathbf{P}_t^{miss}$ . Since the direction of this mismeasurement is random, one should expect the angle  $\phi_{mh}$  to be randomly distributed, as shown on figures 3c and 3d.

Actually, the extraction of the signal from the backgrounds, is based on a cut in the plane ( $\phi_{eh}, \phi_{mh}$ ), not only for the electron channel but also for the muonic and the hadronic channels.

With an expected proton intensity of  $2.4 \cdot 10^{19}$  p.o.t.'s one expects  $1.1 \cdot 10^6$  CC  $\nu_\mu$  interactions and  $3.7 \cdot 10^5$  NC  $\nu_\mu$  events, for the 3 tons target of NOMAD. The following table summarizes for the different  $\tau$  channels the branching ratio (BR), the selection efficiency ( $\epsilon$ ), the number of signal event  $N_\tau$  expected for an oscillation  $\nu_\mu \rightsquigarrow \nu_\tau$  assuming the current limit of  $\sin^2 2\theta = 5 \cdot 10^{-3}$ , the total number of background events  $N_{bkgd}$  for the nominal statistics.

$\tau$ decay mode	BR (%)	$\epsilon$ (%)	$N_\tau$	$N_{bkgd}$
$e^- \bar{\nu}_e \nu_\tau$	17.8	13.5	39	4.6
$\mu^- \bar{\nu}_\mu \nu_\tau$	17.8	3.9	11	2.2
$\pi^- \pi^+ \pi^- \nu_\tau + n \pi^0$	13.8	7.7	18	< 0.2
$\pi^- \nu_\tau$	11.0	1.4	3	< 0.2
$\rho^- \nu_\tau$				
$\rho^- \rightarrow \pi^- \pi^0$	22.7	2.0	7	< 0.2
Total	83.1	28.5	78	$\sim 7$

Table 3: NOMAD sensitivity in the different  $\tau$  decay mode

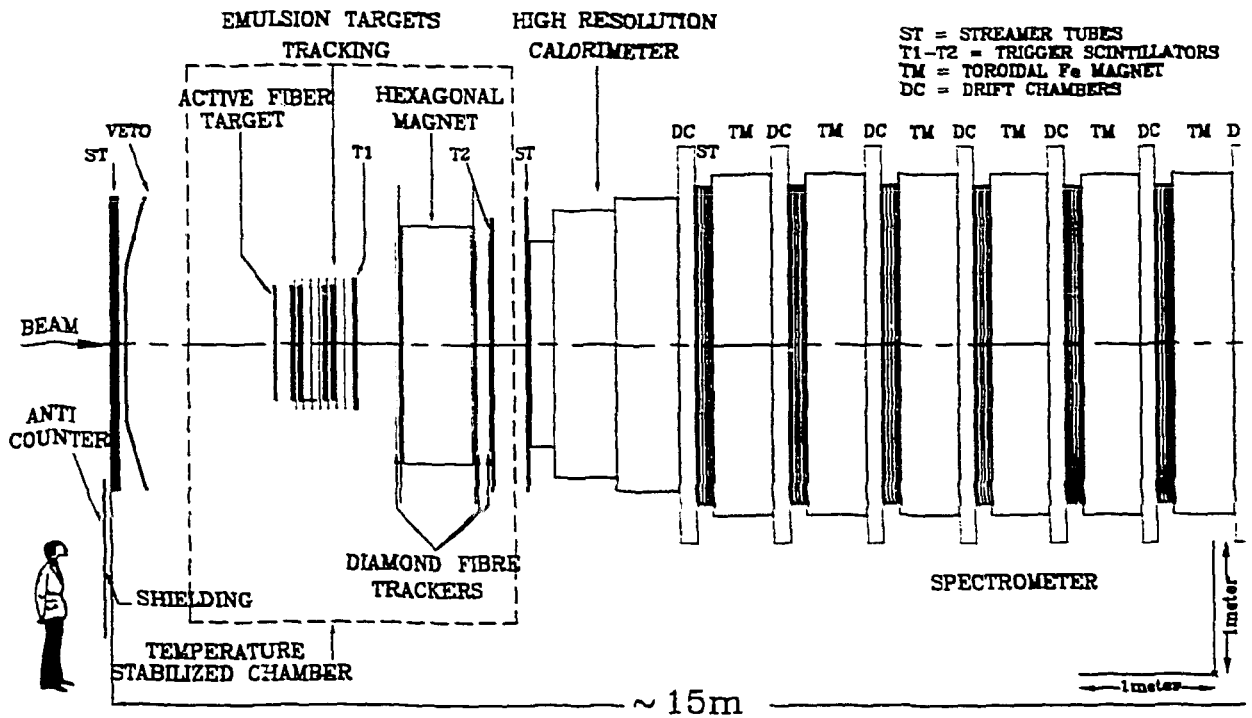
Combining together all the  $\tau$  decay modes listed above gives an overall estimation of the NOMAD sensitivity :

$$\sin^2 2\theta < 3.8 \cdot 10^{-4}$$

at 90% CL for large  $\Delta m^2$ .

### 5.3. CHORUS

The CHORUS<sup>5</sup> (Cern Hybrid Oscillation Research apparatus) detector has been designed to see the  $\tau$  track itself as well as its decay products. The idea is there to use a stack of photographic emulsion (800 kg) where to look for neutrino interactions. In case of  $\nu_\mu \rightsquigarrow \nu_\tau$  oscillation, one expect to find in the emulsion a short track



### EMULSION TARGET

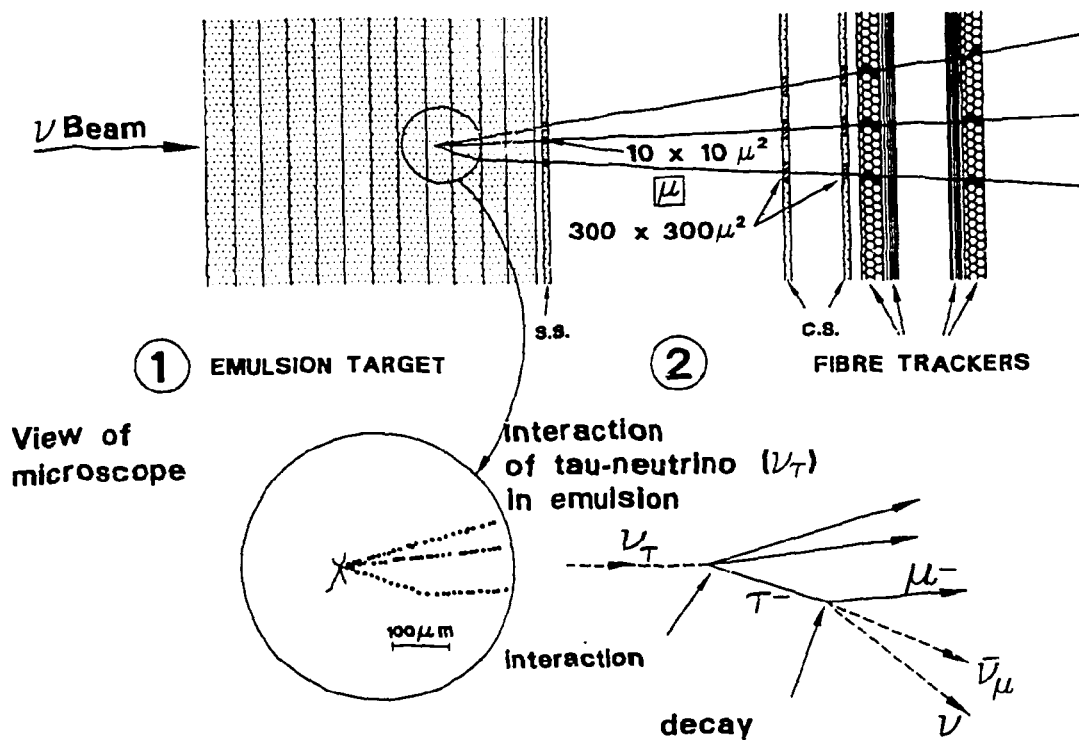


Figure 4: The CHORUS detector

( $\gamma c\tau \sim 1mm$ ) followed by a kink, which would characterise a  $\tau$  decay. According to the very low expected background level, and due to the extraordinary good precision expected on emulsions (few  $\mu m$ ), this method looks very powerful.

### 5.3.1. The detector

The main part of the CHORUS detector (see figure 4) is the bulk of emulsions, grouped in two stacks, separated by a tracking device. This tracking system is a set of three interchangeable emulsion sheets followed by a scintillating fiber array made of ribbons of 250  $\mu m$  in diameter fibers. The tracker is used to determine with a good precision (about 300  $\mu m$ ) a raw impact of the tracks in the changeable emulsion sheets, which are then used to localise the tracks in the emulsion. This localisation of the interactions inside the target, is very important to limit the scanning time to a reasonable value.

The emulsions will be exposed for two years in the neutrino beam. They will be then developed and scanned in different institutes of the collaboration.

Upstream to the target, two large planes of scintillator counters are installed, in order to veto the events aligned with the beam. An additional veto plane is lying on the floor, under the emulsion bulk, for cosmic ray rejection.

After the target an hexagonal magnet is used to measure the track momentum with a resolution varying between 16% ( $p=2$  GeV/c) and 23% ( $p=10$  GeV/c).

In front of the calorimeter a plane of streamer tubes has been installed to help for the pattern recognition.

Besides the energy measurement, which gives a resolution  $\sigma(E_e)/E = 0.13/\sqrt{(E)}$  for electrons and  $\sigma(E_\pi)/E = 0.30/\sqrt{(E)}$  for the hadrons, the calorimeter is used to determine the hadron direction using a center of gravity method.

Finally, a muon spectrometer, from CHARMII, made of six magnetised iron modules, in sandwich with seven drift chambers is used to measure the momentum of the muon tracks.

### 5.3.2. The analysis

The CHORUS experiment would be sensitive to the three following  $\tau$  decay modes :

$$\begin{aligned}\tau^- &\rightarrow \mu^- \bar{\nu}_\mu \nu_\tau \\ \tau^- &\rightarrow \pi^- \nu_\tau \\ \tau &\rightarrow \pi^- \pi^+ \pi^- (n\pi^0)\end{aligned}$$

The first mode is characterised by a muon in the final state. The main background for these events is coming from the  $\nu_\mu$  CC events. For the two remaining modes, with no muon in the final state, the background is mainly due to the NC  $\nu_\mu$  events.

In order to get rid of such CC and NC backgrounds, different criteria are used :

- The CC events are selected by requiring a muon track, which is defined to be either a reconstructed negative track in the muon spectrometer or a negative track stopping in the calorimeter. Few other cuts, like a  $P_t^{miss} > 0.4 \text{ GeV}$ , are also required.
- The NC events are selected by requiring at least a negative track, with energy in the range  $2.5 < E < 10 \text{ GeV}$  which is not recognised as a muon, as defined previously. In addition, a cut  $P_t^{miss} < 2.0 \text{ GeV}$  is applied to enrich the hadronic  $\tau$  sample.

Anyhow, the most convincing feature for  $\nu_\tau$  interaction will be the presence in the emulsion of a track of length between  $30 \mu\text{m}$  and  $3 \text{ mm}$  ending by a kink with an angle greater than  $10 \text{ mrad}$ .

The main backgrounds for the  $\tau$  decay events are the pions scattering inside the target (white stars) and the charm decays.

The table 4 shows for the three different channels, the branching ratio, the selection efficiency, the expected number of events for the current oscillation limits, as well as the background estimations :

$\tau$ decay mode	BR (%)	$\epsilon$ (%)	$N_\tau$	$N_{bkgd}$
$\mu \bar{\nu}_\mu \nu_\tau$	17.7	9.8	23	0.27
$\pi(n\pi^0) \nu_\tau$	49.8	4.6	29	< 0.72
$\pi^- \pi^+ \pi^- (n\pi^0) \nu_\tau$	14.4	6.5	12	< 0.71
Total	81.9	20.9	64	1.7

Table 4: CHORUS selection efficiency and background level

If no event is seen above background, one can deduce a limit on the oscillation  $\nu_\mu \rightarrow \nu_\tau$ :

$$\sin^2 2\theta < 3.1 \cdot 10^{-4} \text{ at } 90\% \text{ CL for large } \Delta m^2$$

## 6. Summary and Outlooks

As presented in the previous sections, new results, in the field of neutrino oscillations, will emerge soon. The neutrino oscillation process still remains one of the best way to look at the neutrino masses. New experimental ideas have been already presented to improve or even to solve the different problems related to neutrino oscillations. In this last section I would like to present some ideas on what will be the future experiments.

### 6.1. Solar neutrinos

The latest results of the GALLEX experiment confirms the initial deficit of solar neutrinos. Beside possible improvements of the solar model, news detectors are

under studies to try to solve the solar neutrino puzzle. The main improvement would be to built *real time* detectors instead of integrated ones, and to lower the threshold on the neutrino energy, in order to get access to the *pp* part of the solar neutrino spectrum. The following table summaries the typical features of new projects :

Detector	Mass (ton)	Material	Threshold (MeV)	Rate (evt/d)
SNO	1000	D <sub>2</sub> O	5.0	2
Super KAMIOKANDE	22000	H <sub>2</sub> O	5.0	49
ICARUS	5000	Liquid Ar	5.0	9
BOREXINO	0.1	Liquid Scintil.	0.25	49
HELLAZ	6	He at 77K	0.1	16

Table 5: New solar neutrino detectors with their characteristics.

### 6.2. Atmospheric neutrinos

The situation about atmospheric neutrinos will be improved soon with the emergence of new experiments sensitive to the allowed region. Most of them are long-baseline experiments, using neutrino beam from accelerators and deep-underground detectors, located far away. It has been proposed to send the KEK PS beam to the (Super)-Kamiokande detector, to send the CERN SPS beam to the Icarus detector, or the the FNAL beam to the Soudan 2 experiment.

The new experiment (P889) is using the high intensity  $\nu_\mu$  beam of the AGS at BNL, which has a mean energy of 1 GeV. The detector would be located at 3 different position (1, 3 and 24 km). It will also improve the situation.

### 6.3. Reactor neutrinos

New proposals, looking for neutrino oscillations at nuclear reactors have been proposed recently. For instance the Chooz experiment, is expected to start data taking next year (1995) before the ignition of the reactor, in order to measure the *true* reactor-off background. The source-detector distance being about 1 km, they will be sensitive to the allowed region for atmospheric neutrinos.

### 6.4. Accelerator neutrinos

The experiment E803 at FNAL, uses technics similar to those of the CHORUS experiment at CERN (emulsions). It has been approved and will start data taking in 1998. Due to the high expected integrated luminosity (about  $10^{21}$  p.o.t's), this experiment will be able to improve by one order of magnitude the NOMAD-CHORUS limit ( $\sin^2 \theta_{\mu\tau} < 3 \cdot 10^{-5}$ ).

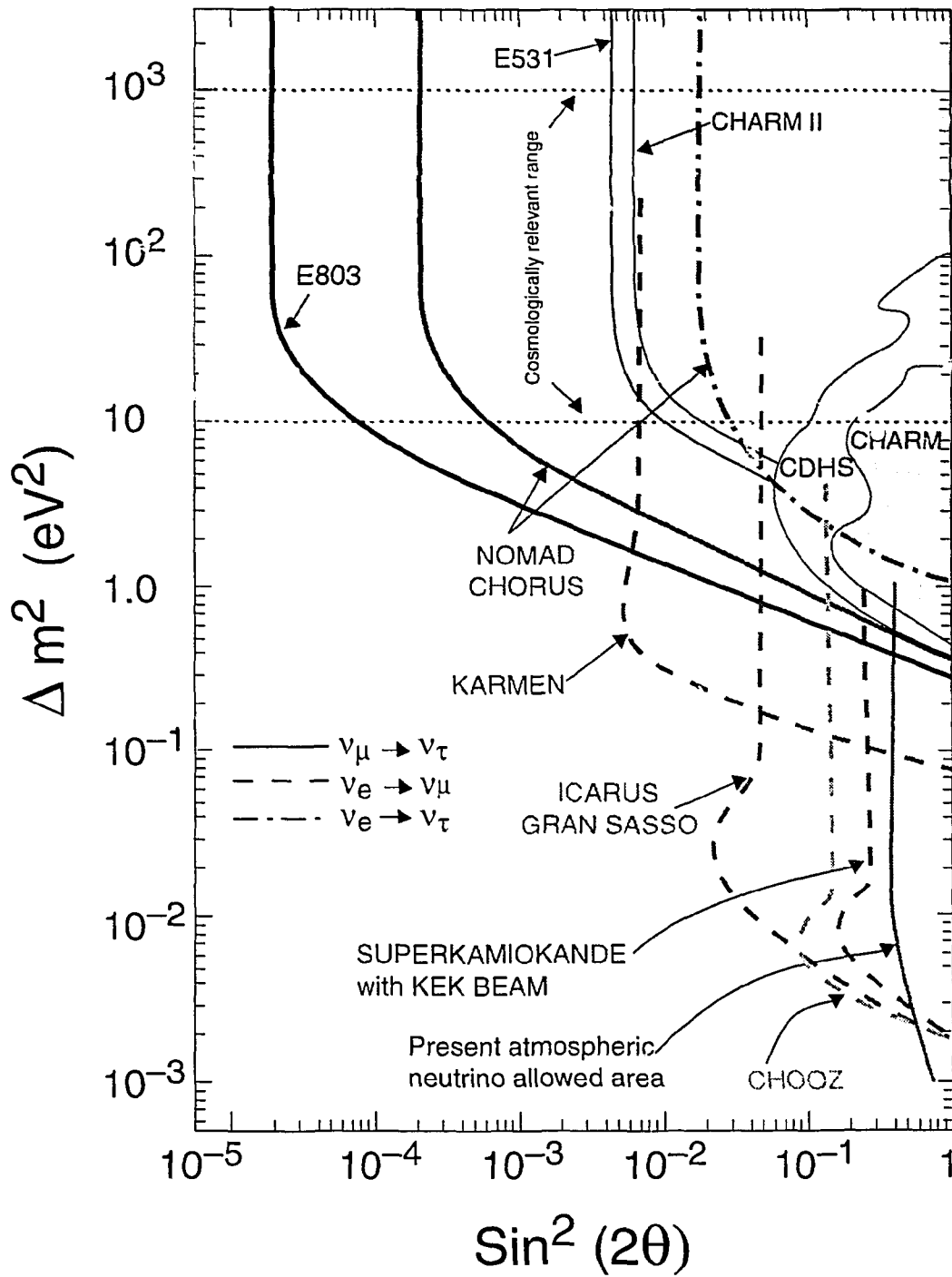


Figure 5: Neutrino oscillations exclusion plot.



By the beginning of the XXI<sup>st</sup> century, it will be possible to use the very intense neutrino beam produced at the LHC collider, either at interaction points in the forward direction along the beam or by using dedicated beam-gas interaction points.

### 6.5. Summary results

The figure 5 summarizes the various exclusion limits discussed in this paper. It shows the region already excluded for the  $\nu_\mu \rightsquigarrow \nu_\tau$  oscillation (shaded area) by the emulsion experiment at FNAL, E531, by CDHS and by CHARM experiments. It also shows the expected limits that can be set by the NOMAD-CHORUS and by the ES03 experiments (solid lines). For the NOMAD and CHORUS, the limit on the  $\nu_e \rightsquigarrow \nu_\tau$  is also shown (dot-dashed line).

The limit set by the KARMEN experiment for the  $\nu_\mu \rightsquigarrow \nu_e$  oscillation is indicated in dashed line.

Also shown on this plot is the allowed region for the atmospheric neutrinos as well as the limits expected for long-baseline experiments (ICARUS and KAMIOKANDE), and by the nuclear reactor experiment CHOOZ.

The solar neutrino region is not represented on that plot.

## 7. Conclusions

The measurements of the neutrinos masses is still an exiting question for physicists. In the coming years it might be possible that unresolved neutrino issues, like atmospheric and solar neutrino problems, find answers. The problem of the dark matter will be investigated by neutrino experiments, and may be part of the puzzle will be solved.

## 8. Acknowledgements

I would like to thank J. Panman for valuable discussions about the CHORUS experiment. Many thanks to my colleagues of NOMAD who gave me the opportunity of this talk, and to B. Ward for his patience.

## 9. Bibliography

1. W. Pauli, remarks at the Seventh Solvay Conference October 1933 *Collected Scientific Papers by Wolfgang Pauli* (Wiley Interscience, New York, 1964) Vol. 2, p 1319.
2. F. Reines and C.L. Cowan, *Phys. Rev.* **92**, 830, 1953.
3. M. Gell-Mann et al., *Supergravity*, Amsterdam, North Holland (1979).
4. NOMAD Collaboration, P. Astier et al., Proposal CERN-SPSLC/91-21 addenda CERN SPSCL/91-48 and SPSCL/91-53.

5. CHORUS collaboration. M. de Jong et al.. CERN-PPE/93-131 (1993)
6. D. Morisson. to appear in the proceedings of the International Conference on Neutrino Physics, Eilat, 1994.
7. E.K. Akhmedov. FTUV/94-9. IFIC/94-6. to appear in the proceedings of the International School on Cosmological Dark Matter, Valencia, 1993
8. Y. Declais. LAPP-EXP-94.08. to appear in the proceedings of the 6th international Workshop on Neutrino Telescope, Venice, 1994.
9. W. C. Louis. to appear in the proceeding of  $\nu$ 's 94, Eilat (1994)